Journal of Physics: Conference Series **443** (2013) 012033 doi:10.1088/1742-6596/443/1/012033

Comprehensive defect characterization of different iron samples after severe plastic deformation

Werner Puff, Xiang Zhou, Bernd Oberdorfer, Boris Scherwitzl, Peter Parz, Wolfgang Sprengel and Roland Würschum

Institute of Materials Physics, Graz University of Technology, Petersgasse 16, A-8010 Graz, Austria

werner.puff@tugraz.at

Abstract. Bulk nanostructured materials produced by means of severe plastic deformation such as high-pressure torsion (HPT) show a high strength in combination with good ductility. These materials exhibit a microstructure down to grain sizes of approximately 100 nm. The defects and microstructure produced by HPT are severely affected by the presence of alloying components. Two iron disks with a purity of about 99.8% (ARMCO) and 99.98+% were deformed by HPT conditioning. Slices of the deformed material were then investigated and subjected to thermal treatment. Upon isochronal annealing at increasing temperatures the decrease of the deformation induced defects was monitored.
The defect structure and its annealing behavior are investigated by positron lifetime spectroscopy and Doppler broadening spectroscopy. In addition specimens were analyzed by high precision difference dilatometry, while the evolution of the microstructure is monitored by electron microscopy. In addition, in situ Doppler broadening measurements upon annealing were performed at the high intensity positron beam at FRM II.
The lifetime data in dependence of the annealing temperature are fitted to a model including positron trapping at grain boundaries and vacancy-type defects.

1. Introduction

Severe plastic deformation (SPD) is one of the promising methods to produce nanocrystalline bulk metals [1, 2]. The benefit of high pressure torsion (HPT) over other methods like, e.g., equal channel angular pressing (ECAP) is the higher strain leading to finer microstructures [3] down to grain sizes of approximately 100 nm [4]. As reported recently, the defects and microstructure produced by HPT are severely affected by the presence of alloying components [5, 6]. This opens up the question, how minor impurities can affect the defect and microstructure of pure metals.

A main feature of nanocrystalline materials is the high concentration of free volumes and their influence on the physical properties. There are a few methods which are specific to study the free volumes associated with lattice defects directly on an atomic level. One method is positron annihilation which has been applied to probe specifically the size of structural free volumes in a variety of nanocrystalline metals prepared by different methods like cluster-condensation or ball milling. Microstructures of pure metals processed by SPD have been widely investigated during the past two decades [7, 8].

Another method, high-resolution difference dilatometry is able to determine directly and specifically the absolute concentration of non-equilibrium excess volumes even in high concentrations by measuring the irreversible macroscopic length change upon annealing. Time-dependent dilatometry [9] supplements the positron annihilation technique, since it enables to study the kinetics of free volumes and vacancies.

2. Experimental

High-purity iron samples (99.98+%) and ARMCO low-purity iron samples (99.8%) were analyzed. One main difference besides others is the lower carbon concentration in pure Fe. Carbon impurities in iron play an important role regarding deformation and structural refinement behavior as well as defect stabilization [10]. The samples, 30 mm in diameter and 10 mm thick, were severely plastically deformed in a high-pressure torsion (HPT) experiment by 10 revolutions applying a pressure of 2.8 GPa. From these deformed disks specimens were cut. The high degree of deformation, given by a van Mises strain of $\varepsilon \sim 36$ was chosen in order to guarantee saturation deformation. According to literature in ARMCO-Fe saturation deformation is reached at an equivalent strain of $\varepsilon = 23$ [11].

For the investigation of the microstructure, scanning electron microscopy (SEM) imaging was performed. For this purpose samples with different annealing states were prepared, namely in the as received state (AR) and after linear heating with 3K/min to different temperatures.

One experimental technique in this paper is differential dilatometry employing a high precision dilatometer (Linseis, L75VD500LT) in vertical setup. This method allows measurements of the irreversible length change due to the annealing of free volumes. With this setup, absolute length changes Δl in the order of 90 nm can be measured accurately, which, in combination with specimen length l in the 10 mm range, gives direct access to absolute measurements of the excess volume concentrations of $3\Delta l/l = \Delta V/V$ down to 3×10^{-5}.

The positron annihilation experiments, lifetime (LT) as well as Doppler broadening (DB) measurements were performed at room temperature in the standard laboratory technique. For the LT measurements a conventional lifetime spectrometer with a time resolution of 190 ps (FWHM) was chosen. The lifetime spectra were analysed using the PFPOSFIT program [12] taking into account a source correction for the annihilation of positrons in the Al foil and the ^{22}NaCl source. For a more detailed analysis of the defect characteristic upon annealing an in-situ measurement by means of the high-intensity positron beam at the NEPOMUC facility at the FRM II in Garching was performed [13].

3. Results and Discussion

For the investigation of the microstructure, scanning electron microscopy (SEM) imaging was performed. For this purpose samples with different annealing states were prepared. The SEM images were analysed with respect to grain size and grain size distribution. The mean grain sizes are 320 nm after HPT processing in pure iron and 150 nm in ARMCO-Fe. In Fig. 1 the micrographs of the samples after HPT deformation in pure iron and ARMCO-Fe are shown.

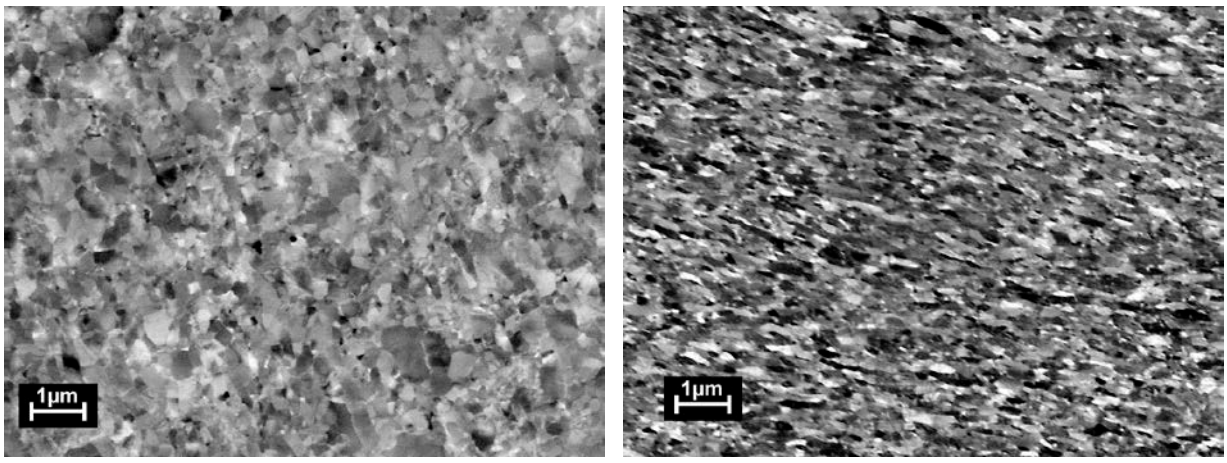

Fig.1 : Scanning electron micrographs after HPT deformation with 10 revolutions of pure Fe (left) and ARMCO-Fe (right).

The grain size distribution of undeformed high-purity Fe and ARMCO-Fe is very similar. However, there are substantial differences in the initial grain size and also the grain shapes after HPT deformation between the high and low impurity samples. While the grains of ARMCO-Fe exhibit a strong lamellar shape, those of HP-Fe are virtual spherical. The larger grain size of HP-Fe can be explained with a dynamic recrystallization during the HPT deformation procedure due to the lack of stabilizing impurities [14]. With higher annealing temperatures the grain structure undergoes coarsening losing also the lamellar structure for the low purity samples. Upon annealing at higher temperatures grain sizes of about 5 µm after temperature treatment at ~ 970 K are obtained.

Fig. 2 shows the grain size obtained from the SEM pictures [15] and the mean positron lifetime at different temperatures. The strong correlation between the grain size and τ_m is evident.

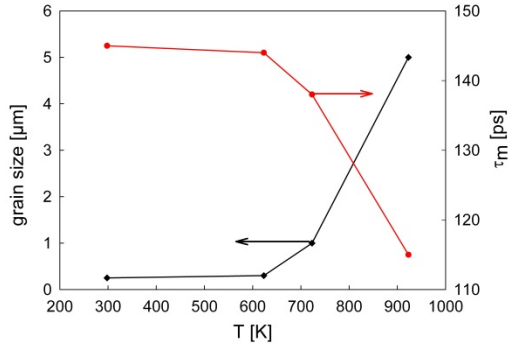

Fig. 2: Grain size and mean positron lifetime at several annealing temperatures for ARMCO-Fe.

For the dilatometric measurements a heating rate of 3K/min was chosen in accordance with the temperature profile of the positron beam measurements (see below). Fig. 3 shows similar annealing characteristics for both samples, however the defect annealing in high-purity Fe starts about 80 K lower and reaches its maximum already at 400 K which is about 100 K less than in ARMCO-Fe. This behaviour can be explained with the different sample purity. Especially the carbon impurities play a crucial role for defect stabilization and recrystallization in iron [10].

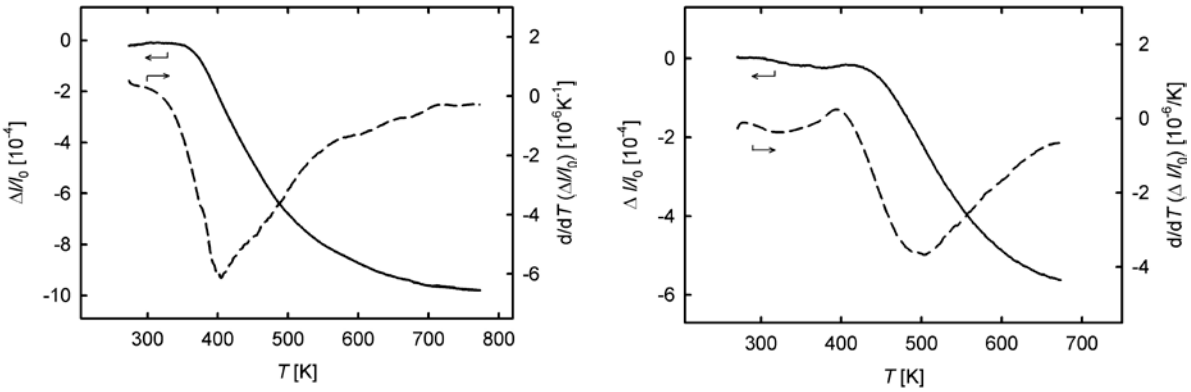

Fig. 3: Dilatometric difference curves of high purity Fe (left). and ARMCO-Fe (right). Also shown are the derivative curves (dashed lines).

Also the different values for the total relative length change are remarkable. The higher total relative length change of nearly 10×10^{-4} in the case of HP-Fe is due to the fact that the overall annealing is shifted to lower temperatures and the maximum annealing temperature applied has even been 100 K higher. The length change results in a relative volume change of about $3\times10^{-}3$. It was discussed

already elsewhere [16], that this volume change exceeds the volume change as expected from the loss of relaxed grain boundaries and dislocations upon annealing-induced crystallite growth. The high volume change, therefore, indicates a high amount of excess free volumes either present as vacancy-type defects and vacancy agglomerates within the crystallites or as excess free volume of unrelaxed grain boundaries.

The ARMCO-Fe samples were also subject to an isochronal annealing for 1 hour in steps of 25 °C from RT to 1025 K. After each annealing step the positron lifetime and the Doppler broadening were measured. Up to 600 K the mean positron lifetime, τ_m, stays constant at 144 ps. After annealing at 625 K τ_m shows a steep decrease from 138 to 118 ps. Above 825 K τ_m scatters around 115 ps. In this temperature range the lifetime spectra can be separated in two components, yielding a defect component with a lifetime of 186 ps and an intensity of about 21%. The lifetime of 186 ps corresponds quite well to the vacancy lifetime in Fe.

The Doppler S-Parameter after isochronal annealing was measured at room temperature for pure Fe as well as ARMCO Fe. In Fig. 4 the obtained ΔS values in dependence of the annealing temperature for both samples are shown ($\Delta S = S - S_{ann}$). Again a temperature shift is observed.

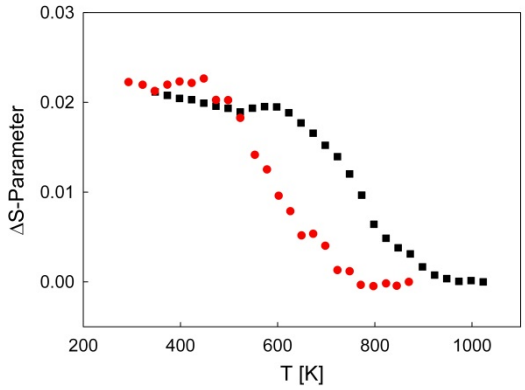

Fig. 4: Difference S-Parameter ΔS as a function of annealing temperature for pure Fe (red dots) and ARMCO-Fe (black squares).

The high number of moderated positrons at the NEPOMUC facility enables studies of fast defect annealing. By choosing the same time profile the results can be combined with dilatometric studies of the annealing of free volumes which are on the same time scale. Fig. 5 shows the difference curve of the S-Parameter of two subsequent measuring runs. Also shown is the resulting relative length change curve. This curve shows a continuous shrinkage from ca. 400 K up to the maximum temperature of 773 K. The annealing characteristics observed by the two complementary techniques of positron annihilation and dilatometry fit together very well. However, a considerable shift of the ΔS-parameter is clearly observable. This shift can be explained with the saturation trapping of positrons at defects for small crystallite sizes [17]. Also shown are the ΔS-Parameter values from isochronal annealing studies. It is obvious that the Doppler data from the two measurements agree quite well.

In a next step the obtained lifetime data for ARMCO-Fe in dependence of isochronal annealing were fitted to a model of competitive positron trapping at point defects within crystallites and diffusion limited positron trapping at grain boundaries [18]. For that purpose values of crystallite diameter in dependence of isochronal annealing were obtained by means of linear interpolation of crystallite sizes measured at selected annealing temperatures (confer Fig. 2).

The experimental data cannot be described by the trapping model when exclusively positron trapping at grain boundaries is assumed, with characteristic values of positron diffusion coefficient, $D_+ = 1\times10^{-4}$ m^2s^{-1}, specific grain boundary trapping rates, $\alpha = 600$ ms^{-1}, free positron lifetime, $\tau_f = 114$ ps, positron lifetime in grain boundaries $\tau_{GB} = 153$ ps.

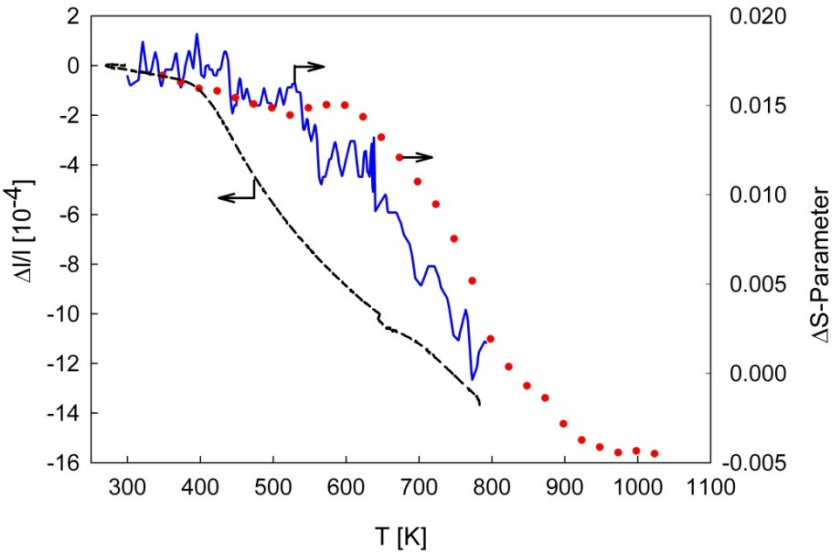

Fig. 5: Doppler broadening ΔS-parameter curve (blue line), dilatometric difference curve (black dashed line) of ARMCO-Fe upon heating with approx. 5K/m and ΔS curve from isochronal annealing (red dots).

The experimental data can only be analysed if in addition to grain boundary trapping vacancy-type positron traps within the crystallites, which anneal in the wake of crystallite growth, are taken into account. The annealing of vacancy-type defects with crystallite growth is simulated with the aid of the well-known theory of Johnson-Mehl-Avrami-Kolmogorov adapted by Henderson for non-isothermal linear heating treatment [19], which has already successfully been applied for describing the recrystallization kinetics in HPT deformed Ni [20]. The pseudo linear heating rate is assumed to be

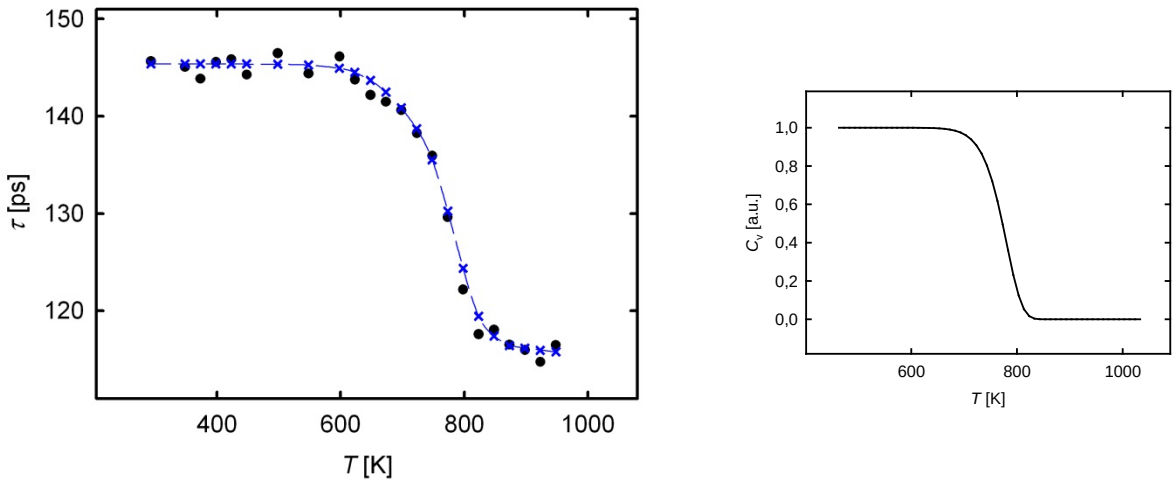

Fig. 6: Fitting of the positron trapping model for grain boundaries and vacancy-type defects to the mean positron lifetime as a function of temperature (left pattern) according to the Henderson model for non-isothermal linear heating treatment (right pattern).

δ = 0.42 K/min. The dependence of the vacancy concentration on temperature is fitted with the following parameters: Activation energy of Q = 1.8 eV, the pre-exponential frequency $\nu = 1\times10^{8}$ s^{-1}, and the Avrami exponent n = 1 (see Fig. 6 right pattern).

With this model of competitive trapping at vacancy-type crystal defects and grain-boundaries, the mean positron lifetime in dependence of annealing temperature can be well described assuming a trap lifetime of 185 ps, an initial concentration of vacancy-type crystal defects $C_{v,\ initial} = 1.4\times10^{-5}$ and a specific positron trapping rate into vacancies $\mu_v = 3\times10^{14}$ s^{-1}.

Vacancy-type crystal defects in iron stable up to temperatures of crystallite growth may be related to carbon impurities. Annealing in the temperature range observed in the present studies was also reported from magnetic measurements of carbon-doped iron after plastic deformation [21].

Acknowledgment

The authors would like to thanks R. Pippan for providing us with the HPT deformed samples, C. Kammerhofer for performing the SEM graphs, Ch. Hugenschmidt for support with the positron measurements at NEPOMUC. Financial support by the Austrian Science Fund (FWF) P21009-N20 is appreciated.

References

[1] Koch C C 2007 *Nanostructured Materials: Processing, Properties and Applications* (New York: Andrews Appl. Sci. Publ.)
[2] Zehetbauer M, Valiev R (Eds) 2004 *Nanomaterials by Severe Plastic deformation* (Weinheim: Wiley-VCH)
[3] Zhilyaev A P, Kim B K, Szpunar J A, Barò M D and Langdon T G 2005 *Mater. Sci. Eng.* A **391** 377
[4] Pippan P, Wetscher F, Hafok M, Vorhauer A and Sabirov I 2006 *Adv. Eng. Mater.* **8** 11
[5] Parz P, Faller M J, Pippan R, Puff W and Würschum R 2012 *Physics Procedia* **35** 10
[6] Bachmaier A and Pippan R 2011 *Mater. Sci. Eng.* A **528** 7589
[7] Krause-Rehberg, Bondarenko V, Thiele E, Klemm R and Schell N 2005 *Nucl. Instr. Methods Phys. Res.* B **240** 719
[8] Cizek J, Janecek M, Srba O, Kuzel R, Barnovska Z, Prochazka I and Dobatkin S 2011 *Acta Mater.* **59** 2322
[9] Ye F, Sprengel W, Wunderlich R, Fecht H-J and Schaefer H-E 2007 *Proc. Natl. Acad. Sci.* **104** 12962.
[10] Vehanen A, Hautojärvi P, Johannson J, Yli-Kauppila J. and Moser P 1982 *Phys. Rev.* B **25** 762
[11] Wetscher F, Vorhauer A and Pippan R 2005 *Mater. Sci. Eng.* A **410-411** 213
[12] Puff W 1983 *Comp. Phys. Commun.* **30** 359
[13] Oberdorfer B 2012 *Doctoral Thesis*, Technical University Graz
[14] Pippan R, Wetscher F, Hafok M, Vorhauer A and Sabirov I 2006 *Adv. Eng. Mater.* **8** 1046
[15] Hohenwarter A, Kammerhofer C and Pippan R 2010 *J. Mater. Sci.* **45** 4805
[16] Oberdorfer B, Lorenzoni, Unger K, Sprengel W, Zehetbauer M, Pippan R and Würschum R 2010 *Scr. Mater* **63** 452
[17] Oberdorfer B, Steyskal E-M, Sprengel W, Puff W, Pikart P, Hugenschmidt C, Zehetbauer M, Pippan R and Würschum R 2010 *Phys. Rev. Lett.* **105** 146101
[18] Oberdorfer B and Würschum R (2009) *Phys. Rev.* B **79** 184103
[19] Henderson D W 1979 *J. Non-Cryst. Solids* **30** 301
[20] Oberdorfer B, Steyskal E-M, Sprengel W, Pippan R, Zehetbauer M, Puff W and Würschum R 2011 *J. Alloys Compd.* **509S** 5309
[21] Refaat A, Farid Z M and Ghobrial F Z 1994 *Z. Phys.* **94** 227